Indian J. Phys. **76A** (4), 361-368 (2002)

IJP A
an international journal

Transport properties of ZnS:Mn at very high electric fields

F M Abou El-Ela
Department of Physics, Faculty of Girls,
Ain Shams University, Heliopolis, Cairo, Egypt

E-mail : Fadlaeg@yahoo.com

Received 28 May 2001, accepted 7 May 2002

Abstract Using ensemble Monte Carlo simulation technique, we have calculated the transport properties of ZnS Mn such as the drift average velocity, the average electron energy and the energy distribution function at very high electric fields. The included scattering mechanisms are polar optical phonon, acoustic phonon, and intervalley phonon , furthermore, a non-parabolic multi-valley model is used Many electrons have energies above 2 1 eV, which represents the threshold energy for Mn impact excitation This fraction of electrons with energies above 2 1 is expected to be 51% and 72% at electric fields of 1.5 and 2 0 MV/cm respectively. No evidence for significant electron population with energy above 5 0 eV is observed, therefore little electron population has enough energy to induce band-band impact ionization The intra-collisonal field effect has a little influence on the electron transport at high fields, though a few electrons execute a Bloch oscillation and collisional broadening

Keywords Ensemble Monte-Carlo, high field transport, hot electron distribution, velocity overshoot, electron-phonon interaction

PACS No. 72 20 Ht

1. Introduction

The wide-band ZnS:Mn has become the most important applied insulator in electroluminescence devices technology [1-3]. It is increasingly used as an active component. The band gap of ZnS Mn is moderately large (3.7 eV at room temperature), but the electron effective mass is small ($m^* = 0.27\, m_0$). The coupling of electrons with optical phonon is not so strong (Frohlich's α = 0 6), therefore, great interest in the charge carrier transport in the material has arisen.

There are two main approaches to treat the transport properties at very high electric fields. The first one, which depends on the mean free path for hot carriers, does not contain any indication to the material band structure except the carrier effective mass [4-8]. These theories are analytical studies that depend on the calculation of the band-band impact ionization scattering rate.

The second approach relies on Monte Carlo simulation method that is a technique of simulation of simultaneous motion of many carriers in *k*-space [8-11]. The Monte-Carlo method allows one to know exactly the carrier momentum at chosen moments of time ; thus, the electron distribution, the average electron velocity, and the average electron energy can be all evaluated. The Monte Carlo technique is a more accurate and exact method, but it requires running a computer program whenever a new condition arises.

To date, there have been many attempts to handle the transport properties of ZnS at very high electric fields. Brennan [12] took care of the full band detail to the first two-conduction bands as well as the full order handling of the electron phonon interaction in ZnS and ZnSe. K. Brennan's results indicated that the distribution function of carriers at 1.0 MV/cm contains an insignificant fraction of carriers at average energy exceeding 2.0 eV; in fact, this was in disagreement with the high efficiency obtained in commercially manufactured thin film electroluminescence devices at the foregoing field.

Transport characteristics of n-ZnS have been calculated by solving the Boltzman transport equation [13]. Mobility of ZnS, which has been given, change from 230 cm^2/V at impurity concentration of $n \approx 10^{19}$ cm^{-3} to 3000 cm^2 / V at impurity concentration of $n \leq 10^{14}$ cm^{-3}.

Bhattacharyya *et al* [14] used a model that covered the first conduction band in non-parabolic three valleys model only. The earlier model did not contain the full band structure or the

Corresponding Author

electron density of states. Despite the above approximation, the steady state electron at high electric fields was enough energetic, but there is no indication for notable electron with energy above 5.0 eV.

Fogarty *et al* [15] have refined a model included a non-parabolic three valleys of the first conduction band and a single valley in second conduction band. Additionally, the density of states was included in the mentioned model through pseudo potential calculation. Important impact on the energy distribution was found after the second conduction band included especially at electric fields above 1 MV/cm. The drift velocity and average electron energy do not differ much from the earlier investigations.

In this work, we used an ensemble Monte Carlo technique to evaluate the transport properties of ZnS:Mn at high electric fields. In our calculation, three non-parabolic valleys model (Γ-X-L) were used. We will show by comparing with other simulations available results [12, 14, 15] and with the generalized lucky drift model [16] that there is no significant loss in physical meaning even in energy range of more than 1 eV compared with the other models which rely on the full band structure.

2. Scattering processes

The most important scattering mechanisms that determine the electron transition in ZnS:Mn at lattice temperature of 300 K are :

(i) polar phonon scattering.

(ii) acoustic phonon scattering.

(iii) equivalent intervalley phonon scattering

(iv) non-equivalent intervalley phonon scattering

We have summarized the most important phonon scattering rates in Appendix 1. The impurity scattering and the piezoelectric phonons scattering were neglected since they are very weak compared to the above scattering mechanisms. However the piezoelectric phonons scattering becomes important only at low lattice temperature in pure piezoelectric semiconductors [17, 18]. At this stage, we have ignored the impact ionization processes despite its importance at high electric fields in our present calculation [12, 15, 19]. This approximation is mainly due to a vast amount of computer resources needed to run the simulation program.

The screening of polar mode interaction was also neglected due to lower carrier concentration in our investigation. In addition, the admixture of p-type wave function of conduction band was neglected at electron energy exceeding 1.0 eV.

3. Monte Carlo model

The Monte Carlo method makes the solution of Boltzmann transport equation possible by the use of a statistical numerical approach. This approach follows the transport history of one or more carriers which are subject to the action of external forces. These forces which affect the particles consist of an applied field and scattering mechanisms. The method of Mote Carlo (MC) technique generates sequences of random numbers with specified distribution probabilities. These probabilities are used to describe quantities such as scattering events which determine the time between successive collisions of carriers [9-11, 20].

The Monte Carlo simulation requires a detailed definition of the physical system as a starting point. The electron transport in a semiconductor requires material parameters, knowledge of energy band structure, lattice temperature and a definition of the applied electric field. The process of simulating the electron motion involves a number of computational steps to calculate the duration of each free flight, select the scattering mechanisms at the end of the flight and determine the final wave vector of the scattered electron.

The state of an electron is specified by its wave vector k which is related to the electron energy E and the electron velocity in non-parabolic conduction bands by

$$E(1+\alpha E) = \frac{\hbar^2 k^2}{2m^*}$$

$$v = \frac{1}{\hbar}\frac{\partial E}{\partial k},$$

where α is the band non-parabolicity factor and electron effective mass in the material.

The probability of duration of a free flight time is

$$g(t) = \lambda[k(t)] \exp\left[-\int_0^t \lambda[k(t')]dt'\right]$$

$\lambda[k(t)]$ is defined as the total scattering rate for electron of wave vector $k(t)$, in which $\lambda(k) = \sum_i^s \Gamma_i(k)$, $\Gamma_i(k)$ is the scattering rate due to the ith process and s is the number of scattering processes. In eq. (3), $\lambda[k(t)]$ represents the electron probability of scattering at time t, where as $\exp\left[-\int_0^t \lambda[k(t')]dt'\right]$ is the probability that the electron survives without suffering a scattering in interval t.

The free flight is related to the total scattering rate due to all the operative mechanisms and the inclusion of a fictitious self scattering term which is necessary to keep the total scattering rate constant. ($\Gamma = \lambda(k) + \lambda_{self}$ where λ_{self} is self-scattering rate). Self-scattering is a virtual process, which leaves the state of an electron, unchanged and is only included to keep the calculation of the free flight time simple to determine [9, 10, 20].

The free flight duration time is given by

$$t = \frac{1}{\Gamma}\ln(1-r_1),$$

where Γ is the total scattering rate and r_1 is a random number distributed between (0, 1) and is provided by the computer library. The motion of the electron in an electric field F is given by

$$k(t) = k_0 + \frac{eF\,t}{} \tag{5}$$

where e is the electron charge, t is the free flight time, and k_0 is defined as the wave vector at time $t = 0$.

The choice of the scattering mechanism is to be determined at the end of the free flight by generating a second random number r_2 in the range $1 \geq r_2 \geq 0$. The scattering processs is selected if

$$\sum_{i=1}^{i-1} \Gamma_i(k) \leq r_2 \leq \sum_{i=1}^{i} \Gamma_i(k) \tag{6}$$

The choice of the scattered wave vector requires the following

(i) calculation of the magnitude of the scattered wave vector according to $k' = (2m^*E')^{\frac{1}{2}} / \hbar$ where E' is the electron energy after the scattering with the phonon

(ii) the use of the quantum mechanical expression of the probability formula for the scattering angle . We can select the angle by generating third uniform random number r_3 distributed between (0,1), according to

$$\frac{\int_0^{\theta} p_i(\theta)\, d\theta}{\int_0^{\pi} p_i(\theta)\, d\theta}. \tag{7}$$

(iii) obtaining the azimuthal angle directly by fourth random number r_4 distributed between (0, 1)

$$\varphi = 2\pi r_4 \tag{8}$$

The wave vector is then modified according to the physical nature of the chosen phonon process, in this way, the final state of electron is determined. The momentum and energy of electron is updated and is allowed to continue its flight until it is again terminated by scattering according to eq.(4).

In Ensemble Monte Carlo method [10, 11, 20] an ensemble of N electron states are chosen randomly, with Maxwellian distributions at start of simulation, the N electrons are simulated in parallel. The required time of simulation divided into equal intervals DT for the number of steps. Thus, all the N electron states are completely known at the end of every step. It is recommended to make N as large as possible in order to reduce the statistical fluctuation $\left(\approx \frac{1}{\sqrt{N}}\right)$. We might keep in our consideration the available storage memory and the computer time allowed.

When the electric field is applied in the x direction, the average drift velocity and the average electron energy are given respectively by

$$\bar{v}_d = \frac{1}{N}\sum_{i=1}^{N} v_i(t), \qquad \bar{E} = \frac{1}{N}\sum_{i=1}^{N} E_i(t), \tag{9}$$

where

$$v_i(t) = \frac{\hbar k_x}{m^*(1+2\alpha E_i)}, \qquad E_i(t) = \frac{-1+\sqrt{1+4\alpha\gamma(k)}}{2\alpha}$$

and

$$\gamma(k) = \frac{h^2}{2m^*}\left(k_x^2 + k_y^2 + k_z^2\right). \tag{10}$$

The sum in eq. (9) is over all N electrons, $v_i(t)$ and $E_i(t)$ represent the electron drift velocity and the electron energy respectively at the end of each step, while k_x, k_y and k_z are the wave vector components in x, y and z directions for each electron respectively.

The distribution function (D.F) is determined by setting up at the start of simulation a histogram of k space, the number of electrons visiting each finite cell for each valley are accumulated throughout the calculation. The electron distribution function is directly proportional to the number of electrons in each finite cell.

4. Results and discussion

Figure 1 shows the calculated scattering rate for phonons in Γ valley of ZnS : Mn at 300K. The reference Figure shows how

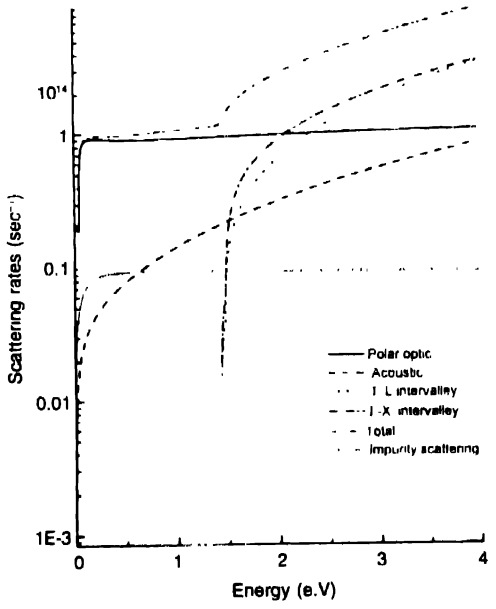

Figure 1. Scattering rates *versus* electron energy in Γ valley of ZnS:Mn at 300K.

small acoustic phonon scattering was. In fact, the principle scattering source is mainly due to optical type phonons either through polar interaction or through intervalley deformation potential interaction. We may note that the high energy of electrons in upper valley interact with phonon mainly through the deformation potential since the polar interaction falls off with increasing electron energy.

The calculated drift velocity *versus* electric field for ZnS:Mn at 300 K is shown in Figure 2. We also displayed in the earlier Figure our analytical velocity model, in addition to the results of Brennan [12] and Bhattacharyya [14] for comparison. In our analytical velocity model, we adopted a particular form for the average drift velocity *versus* the electric field [8]

$$V = V_S\left[1-\left(1-3.25\times10^{-5}F\right)\exp\left(-0.75\times10^{-6}F\right)\right], \quad (11)$$

where F is applied electric field. V_S is the electron saturation velocity which could be estimated from Monte Carlo results to be 0.7×10^7 cm/sec at very high electric fields. Indeed, eq. (11) represents rough estimation for what may be expected for electron velocity in ZnS · Mn.

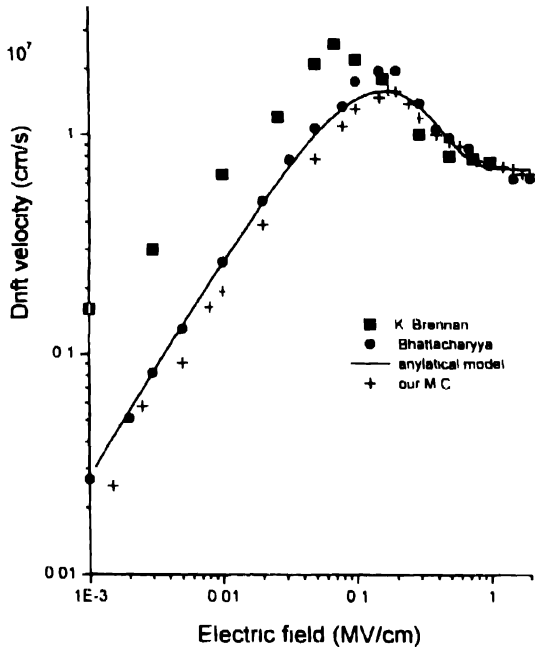

Figure 2. Steady-state drift velocity *versus* electric field for ZnS:Mn at 300K.

It is obvious that the threshold field for intervalley transfer in Brennan's results were much smaller than what be deduced from both our M.C results and Bhattacharyya's results. In fact, it is understood that the threshold field depends on the strength of polar optical phonon scattering and the effective mass in valleys. However, on all the previous calculation, the same strength of polar optical phonon scattering rate and the same electron effective mass (0.28 m_0) have been used.

Our Monte Carlo calculation of steady state average velocity curve was in a good agreement with all other previous results at very high electric fields but it deviated at low fields. The analytical model results agreed quite well with those obtained by Bhattacharyya *et al* at low field. Nevertheless, it deviated at threshold electric field. On the other hand, the analytical model results agreed quite well with our Monte Carlo results at both threshold electric field and high electric fields region ; however, it differed at low electric field region. The mobility at electric field of 1MV/cm was found 80 cm^2/V. Meanwhile, the polar optical phonon, the deformation phonon, and the intervalley phonon were included.

The calculated low field mobility of ZnS agreed with the experimental data that varied in the range of (80-300 cm^2/V) [21] Moreover, there is evidence that threshold field for intervalley transfer in our results was the same as obtained by Bhattacharyya *et al.*, but it was nearly twice the value obtained by Brennan. Bhattacharyya *et al* attributed the discrepancy because of the large low-field mobility in Brennan's results that was unrealistic if it is compared with the experimental low field reported data.

In Figure 3, the standard-average energy field was compared with Bringuier's results [16], which are obtained in the framework of generalized lucky drift model and a Monte Carlo simulation included a full band structure. For more details the reader is referred to reference [16]. The mentioned Figure showed the average energy E_{av} using the generalized lucky drift model demarcation energy $E_{\frac{1}{2}}$, for which $P(E_{\frac{1}{2}}) = \frac{1}{2}$ in the generalized lucky drift model, and the average energy using our Monte Carlo method for a comparison as function of the electric field. At low fields, our calculated simulation results agreed qualitatively with E. Bringuier's results. Therefore, this is evidence of validity of our approximation, in the limit of low

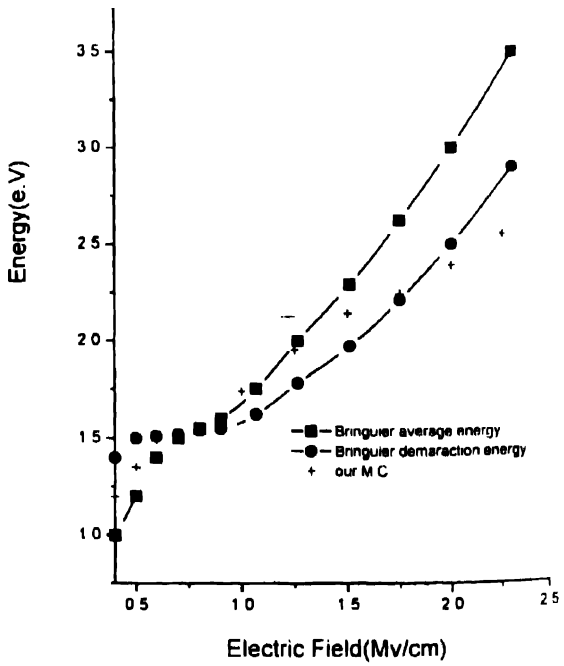

Figure 3. Average electron energy *versus* electric field.

fields. On contrary, our simulation results differed significantly, from what was reported by Bringuier at high fields (above 1.0 MV/cm). However the results obtained for the average energies at 1.0, 1.5 and 2.0 MV/cm are compared remarkably well with the available Monte Carlo results [14, 15].

Figure 4 showed the sum of electron population in three different valleys for applied electric fields (1.0, 1.5, and 2.0 MV/cm) *versus* an electron energy. The mentioned results clearly indicated that the peak of distribution shifts towards high energy as the electric field increases due to the high field heating. The electron distribution was found to be localized in the neighborhood of threshold energy, which for the impact ionization of manganese center is approximately 2.1 eV.

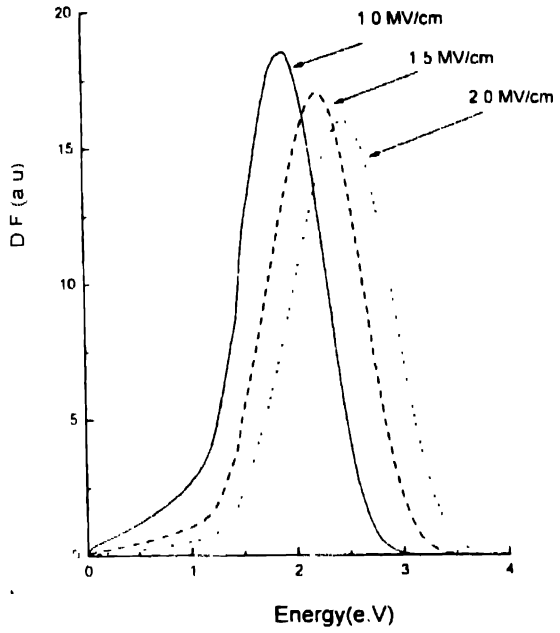

Figure 4. Steady-state electron distribution as a function of energy

We estimated the percentage number of electron exceeding 2.1 and 3.2 eV; however, the latter corresponds to the approximate threshold energy for the blue emission. Table 1 summarized the percentage number of electrons above 2.1eV at various electric fields reported by Brennan's M.C simulation, Bringuier's lucky-drift model, Bhattacharyya's M.C simulation and our M.C simulation. Moreover, Table 2 represented the percentage number between 2-1 and 3·2 eV for the Bhattacharyya's M.C simulation and our M.C simulation. In both Tables, our M.C simulation results were quite comparable with the other results at 1.0 and 1.5 MV/cm; however, there is large difference at 2.0 MV/cm.

Table 1. Percentage number of electrons above 2 1 eV

Electric field (MV/cm)	brennan	Bringuier	Bhattacharyya	our
1	1%	19%	26%	22.5
1 5	–	–	50%	52%
2	-	66%	65%	72%

Table 2. Percentage number of electrons between 2 1 and 3 2 ev

Electric field (MV/cm)	Bhattacharyya	our
1	26%	22%
1 5	50%	51%
2 0	54%	69%

The percentage number of electrons between 2.1 and 3.2 eV (for which the impact excitation cross section is significant) was estimated to be 22%, 51% and 69%.

In the Bhattacharyya's M.C simulation result, they are 26%, 50% and 54% at electric fields 1.0, 1.5 and 2.0 MV/cm respectively.

In Figure (5a-b), the number of electron energy distribution function, $n(E)$, was shown for electron in Γ valley, L valley,

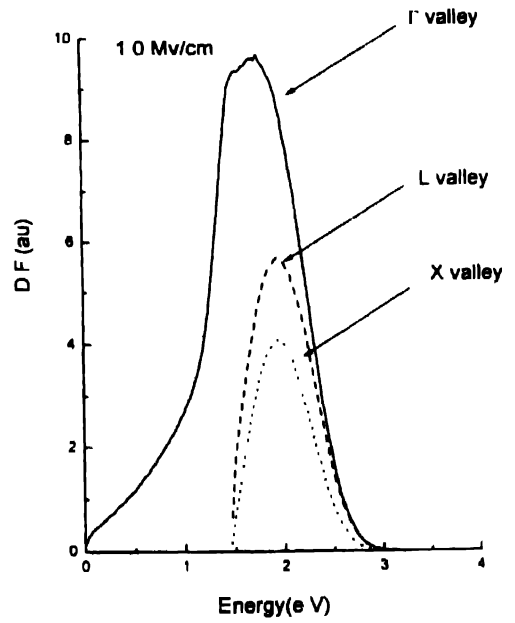

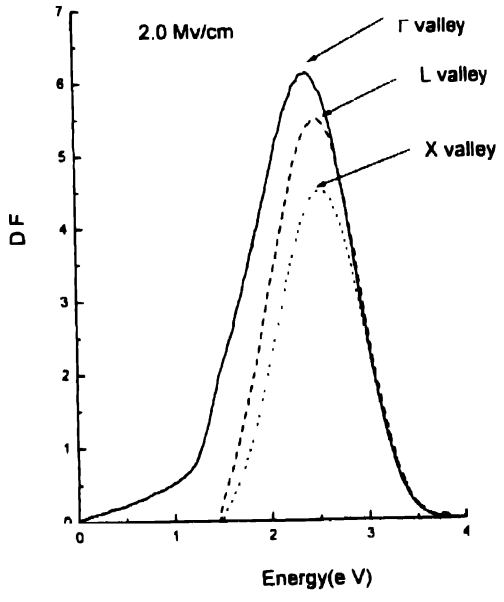

Figure 5(a-b). Steady-state electron energy distribution as a function of electron energy in each of the three valleys

and X valley at electric fields 1.0 and 2.0 MV/cm respectively. In this study, the electric field was chosen to agree with a typical field for ACTEFEL electroluminescent devices. It could be seen from the previous Figures that the electron distribution in both L and X valleys are comparable with the Γ valley at field 2.0 MV/cm while it was smaller at 1.0 MV/cm.

The distribution function did not have many different features from that obtained by Bhattacharyya *et al.* where the tail of the distribution ends at electron energy less than 4.0 eV at electric field of 2.0 MV/cm.

The time variations of the average electron energy and the electron occupancy in each valley are given in Figure 6 and 7 respectively. The total weighted average was also included in both earlier Figures. In both Figures, the applied electric field was chosen as 1.5 Mv/cm. The dynamic properties have been obtained by assuming that all these electron were initially in the Γ valley. After a short period (equal in this case to energy relaxation time), only about 50% of electrons transfer to the L and X valleys, this mean a significant fraction of electrons have energy in excess these of Mn-luminance excitation. Also Figure 6 shows electron energy runaway in which a fraction of the electrons gains energy from the field at a faster rate than energy dissipate to the lattice. This energy runaway occurs as a consequence, of ignoring the band-band impact ionization which becomes very important at the field of 1.5 MV/cm [22].

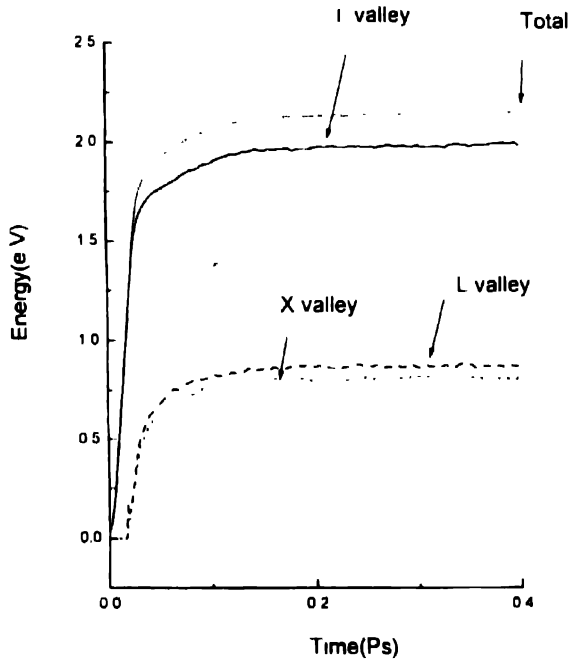

Figure 6. Time dependence of the average electron energy at electric field 1.5 Mv/cm in each of the three valleys.

Although, we have reached the end of our study, we are still far from understanding the electron transport in ZnS:Mn at very high fields. Our results have shown that at the high fields, the electron energy varies in the range (1-2 eV), which corresponds to the variation of electron scattering rate ($1 \times 10^{14} - 4 \times 10^{14}$ s^{-1}). The theory of electron transport in the above mentioned electron energy faces the following difficulties :

(i) Quantum effects such as intra-collision field effect and collisions broadening need to be tackled.

(ii) Electrons oscillate between band edges before scattering. Electrons executing Bloch oscillation may scatter and drift quite differently from free electrons.

(iii) Electrons scattered all over the Brillouin Zone and inclusion of realistic band structure are expected to expand our understanding of high field transport.

(iv) A Hot phonon effect is essential at high electron energy.

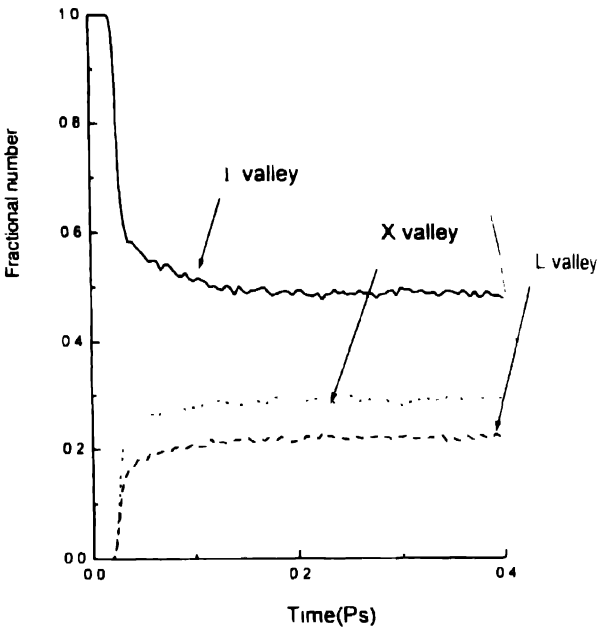

Figure 7. Time dependence of the electron fractional occupancy at electric field 1.5 Mv/cm in each of the three valleys.

First, let us examine the so called intra-collision field effect. Collision may occur so frequently that it begins before the last collision ends. Suppose that the collision must take time τ_c. This time is roughly $\frac{\hbar}{E}$, where E is electron energy so that for 2eV electron, $\tau_c = 3.3 \times 10^{-16}$ s, whereas the scattering rate $\lambda = 4 \times 10^{14}$ s^{-1}, provided

$$\lambda \tau_c = 0.013 < 1.$$

Therefore, it is safe to ignore the intra-collisional field effect in Zns:Mn while the first order perturbation theory is still valid. During the collision period 3.3×10^{-16}s, electron will travel distance ≈ 0.5 Å in a field of 2.0 M/cm.

The collisional broadening energy associated with phonon is written as $\Delta E = \frac{\hbar}{\tau}$ [23], where ΔE is the change in energy and $\frac{1}{\tau}$ is the scattering rate in ZnS : Mn. At the field 1MV/cm.

ΔE is equal to 6.5 meV, while, it is 30 meV at 2MV/cm. This ΔE is still small in comparison with the electron energy 2.0eV, but it is larger than phonon energy. Therefore, collisional broadening energy associated with the phonon collision is safe to neglect in high field transport until 1 MV/cm but it becomes questionable at 2 MV/cm. This may be the reason why our M.C result differs from the generalized lucky drift model at this field in Figure 4.

Consider the possibility of Bloch oscillation, the angular frequency (ω_b) is given by $\frac{eFa}{\hbar}$, where a is the lattice constant. If the scattering time is τ, then Bloch oscillation will occur if $\omega_b \tau > 1$ [18]. For the maximum field 2 MV/cm and taking a=5.4 Å, we calculate $\omega_b = 1.6\times10^{14}$ s^{-1}. The scattering rate according to Figure 1 is approximately equal to 4×10^{14} s^{-1}, consequently, $\omega_b\tau = 0.4$. We have to conclude that Bloch oscillation are not likely to be important at high field in Zns : Mn Although a few number of electrons may execute Bloch oscillations.

5. Conclusion

An ensemble M.C simulation for the high fields in ZnS:Mn has been developed including all the relevant scattering mechanisms. At field of the order of 1Mv/cm, a significant number of the electron population has the energies of the threshold for Mn luminescence excitation (2.1 eV). This fraction of electrons with energies above 2.1 is expected to be 51% and 72% at electric fields of 1.5 and 2.0 MV/cm respectively. At the same time, no evidence for significant electron population with energy above 3.0 eV is observed ; therefore, little electron population has enough energy to induce band-band impact ionization. Our transport properties in ZnS:Mn at very high fields showed a good agreement with the lucky drift model and the other published data. Although a few numbers of electrons may execute Bloch oscillations, the vast majority will not. The intra-collisional field effect is safe to ignore at high field; however, collisional bradening effect becomes important to be included at 2.0 MV/cm.

Acknowledgments

The author would like to thank professor M A Kenawy, Aim Shams University, for helpful discussion and for critical reading of this manuscript.

References

[1] D Pryce *Electron Display World* **33** 138 (1988)
[2] J W Allen *J Phys* **C19** 6287 (1988)
[3] M Beale *Phil. Mag.* **B68** 573 (1993)
[4] P A Wolff *Phys. Rev* **95** 1415 (1954)
[5] W Shockley *Solid State Electron* **2** 35 (1961)
[6] G A Barf *Phys. Rev.* **128** 2507 (1962)
[7] B K Ridley *J. Phys.* **C16** 3373 (1983)
[8] B K Ridley and F A El-Ela *J Phys. Condens. Matter* **1** 7021 (1989) ; *Solid-State Electron* **32** 1393 (1989)
[9] W Fawcett, A D Boardman and S Swain *J. Phys. Chem. Solids* **31** 1963 (1970)
[10] C Jacoboni and L Reggiani *Rev Mod Phys* **55** 645 (1983)
[11] F M Abou El-Ela, *Ph D Thesis*, (Essex University, England) (1989)
[12] K Brennan *J Appl. Phys* **64** 4024 (1988)
[13] H E Ruda and B Lai *J Appl. Phys* **68** 4 (1990)
[14] K Bhattacharyya, S M Goodnick and J F Wager *J. Appl Phys* **73** 3390 (1993)
[15] J Fogarty, W Kong and R Solanki *Solid State Electron* **38** 3 653 (1995)
[16] E Bringuier *Phys Rev* **49** 7974 (1994)
[17] B R Nag *Electron Transport in Compound Semiconductors* (Berlin Springer-Verlag) (1980)
[18] B K Ridley *Quantum Processes in Semiconductors* (Oxford Clarendon) (1988)
[19] M Reigrotzki, R Redmer, I Lee, S Pennathur, M Dur, J F Wager, S M Goodnick, P Vogl, H Eckstein and W Schattke *J Appl. Phys* **80** 5054 (1996)
[20] R W Hockney and J W Eastwood *Computer Simulation Using Particles*, (Bristol : Adam-Hilger) (1988)
[21] W E Spear and P G le Comber *Phys Rev Lett* **13** 434 (1964) , P G le Comber, W E Spear and A Weinmann *J Appl Phys* **17** 467 (1966)
[22] W M Ang, S Pennathur, L Pham, J F Wager, S M Goodnick and A A Douglas *J Appl Phys* **77** 2719 (1995)
[23] F Capasso *Semiconductors and Semimetals* **22D** 1 (1986)

Appendix 1

This appendix lists the important kinds of different phonons scattering rates used in the Monte Carlo method, assuming non parabolic bands at the lattice temperature T. For more details of these scattering rates, the reader is referred to the References [9-11, 17].

(i) Acoustic phonon scattering rates

This interaction of the acoustic phonon is due to the deformation potential and is given by

$$\Gamma_{ac}(k) = \frac{(2m^*)^{1/2} k_B T}{2\pi \rho s_v^2 \hbar^4} \Xi_a^2 \gamma^{1/2}(E)(1+2\alpha E) F_a(E), \quad \text{(A1)}$$

where $\gamma(E) = E(1+\alpha E)$, and

$$F_a(E) = \frac{(1+\alpha E)^2 + 1/3(\alpha E)^2}{(1+2\alpha E)^2}$$

Ξ_a, ρ and S_v represent the acoustic deformation potential, the specific mass density of crystal and the sound velocity. α is the nonparabolicity factor.

(ii) Polar optical phonon scattering rates

The scattering rate due to the polar optical phonon is evaluated as

$$\Gamma_{po}(k) = \frac{e^2 m^{*1/2} \hbar\omega_{po}}{4\sqrt{2}\pi\varepsilon_0 \hbar^2}\left(\frac{1}{\varepsilon_\infty} - \frac{1}{\varepsilon_s}\right)\frac{1+2\alpha E'}{\gamma^{1/2}(E)}$$

$$F_0(E,E')\times\left(N_{po}+1/2\pm1/2\right), \tag{A2}$$

where N_{po} is the optical phonon occupation number, which is given by Bose Einstein statistics. The ± sign refers to phonon emission or absorption respectively. $\hbar\omega_{p0}$, ε_s, ε_∞ and ε_- represent the energy of polar optical phonon, the relative static dielectric constant, the high frequency dielectric constant and the permittivity of free space respectively.

In the above equation, we use the following notation

$$\gamma(E')=E'(1+\alpha E'),$$

$$F_0(E,E')=C^{-1}\left|A\ln\frac{\gamma^{1/2}(E)+\gamma^{1/2}(E')}{\left|\gamma^{1/2}(E)-\gamma^{1/2}(E')\right|}+B\right| \tag{A3}$$

$$A=\left[2(1+\alpha E)(1+\alpha E')+\alpha\left(\gamma(E)+\gamma(E')\right)\right]^2,$$

$$B=-2\alpha\gamma^{1/2}(E)\,\gamma^{1/2}(E')\left[4(1+\alpha E)(1+\alpha E')+\alpha\left(\gamma(E)+\gamma(E')\right)\right],$$

$$C=4(1+\alpha E)(1+\alpha E')(1+2\alpha E)(1+2\alpha E').$$

(iii) Equivalent intervalley phonons scattering rates

We shall consider equivalent Intervalley phonon scattering in the X, L bands only, the Intervalley scattering rate for all possible transition between equivalent valleys is given by

$$\Gamma_e(k)=(Z_e-1)\frac{m^{*3/2}D_e^2}{\sqrt{2}\pi\hbar^3\rho\omega_e}\gamma^{1/2}(E')(1+2\alpha E')\times\left(N_e+1/2\pm1/2\right), \tag{A4}$$

where ω_e is the equivalent intervalley phonon frequency, D_e is the deformation potential for the equivalent intervalley scattering, Z_e is the number of equivalent valleys and N_e is the equivalent intervalley phonon occupation number, which is given by Bose Einstein statistic.

(iv) Non-equivalent intervalley phonons scattering rates

In high electric fields, the electron energy in ZnS may become sufficiently high, so electron scatter into the L, X valley. The intervalley scattering rate between non-equivalent valleys is given by

$$\Gamma_{ij}(k)=Z_j\frac{m_i^{*3/2}D_{ij}^2}{\sqrt{2}\pi\hbar^3\rho\omega_{ij}}\gamma^{1/2}(E')(1+2\alpha E')\times\left(N_{ij}+1/2\pm1/2\right), \tag{A5}$$

where ω_{ij} is the intervalley phonon frequency, D_{ij} is the deformation potential for non-equivalent intervalley scattering, Z_j is the number of valleys of type j and N_{ij} is the intervalley phonon occupation number, which is also given by Bose Einstein statistic. The electron energy is measured from the minimum of valley which are situated at energies Δ_i and Δ_j for valleys i and j, respectively, while $\hbar\omega_{ij}$ is the energy of the phonon involved

$$E'=E_i-\Delta_j+\Delta_i+\hbar\omega_{ij}\,,\quad \text{phonon absorption}$$

$$E'=E_i-\Delta_j+\Delta_i+\hbar\omega_{ij}\,,\quad \text{phonon emission}$$

Apendix 2

Free flight times generation

The procedure used to generate random free flight time t with a probability distribution ($g(t)$) given by eq. (3) from a random number r_1 with uniform probability distribution $P(r_1)$ in the range (1, 0) is as follows [9, 10, 20]. Since

$$P(r_1)dr_1=g(t)\,dt\,, \tag{B1}$$

then

$$\int_0^{r_1}p(r_1')\,dr_1'=\int_0^t g(t')dt'$$

which upon integration, gives

$$r_1=\int_0^t g(t')dt'. \tag{B2}$$

This can be written as

$$r_1=1-\exp\left[-\int^t\lambda\left[k(t')\right]dt'\right. \tag{B3}$$

Obviously the expression (B3) is not easy to solve, and this is where self-scattering comes in. The idea is to introduce a non-negative transition rate λ_{self} for the null process. When the self-scattering is included among the scattering mechanisms the total scattering rate Γ is a constant for all k vectors ($\Gamma=\lambda(k)+\lambda_{self}$).

Then we can evaluate the integral in eq. (B3) and obtain an expression for t as a function r_1

$$r_1=1-\exp(-\Gamma t)$$

or

$$t=-\frac{1}{\Gamma}\ln(1-r_1). \tag{B4}$$